HHS Public Access

Author manuscript

J Immunol. Author manuscript; available in PMC 2018 September 01.

Published in final edited form as:

J Immunol. 2017 September 01; 199(5): 1748–1761. doi:10.4049/jimmunol.1700472.

Manipulating glucose metabolism during different stages of viral pathogenesis can have either detrimental or beneficial effects

Siva Karthik Varanasi[*], **Dallas Donohoe**[¶], **Ujjaldeep Jaggi**[‡], and **Barry T Rouse**[*,‡,#]

[*]Department of Genome Science and Technology, University of Tennessee, Knoxville, Tennessee

[‡]Department of Biomedical and Diagnostic Sciences, College of Veterinary Medicine, University of Tennessee, Knoxville, Tennessee

[¶]Department of Nutrition, College of Education, Health & Human Sciences, University of Tennessee, Knoxville, Tennessee

Abstract

This report deals with physiological changes and their implication following ocular infection with herpes simplex virus (HSV). This infection usually results in a blinding inflammatory reaction in the cornea orchestrated mainly by pro-inflammatory CD4 T cells and constrained in severity by regulatory T cells (Treg). In the present report, we make the unexpected finding that blood glucose levels change significantly during the course of infection. Whereas levels remained normal during the early phase of infection when the virus was actively replicating in the cornea, they increased around two fold during the time when inflammatory responses to the virus was occurring. We could show that glucose levels influenced the extent of induction of the inflammatory T cell subset in vitro that mainly drives lesions, but not regulatory T cells. Additionally, if glucose utilization was limited in vivo as a consequence of therapy in the inflammatory phase with the drug 2DG, lesions were diminished compared to untreated infected controls. In addition, lesions in 2DG treated animals contained less pro-inflammatory effectors. Glucose metabolism also influenced the acute phase of infection when replicating virus was present in the eye. Thus, therapy with 2DG to limit glucose utilization caused mice to become susceptible to the lethal effects of HSV infection, with virus spreading to the brain causing encephalitis. Taken together, our results indicate that glucose metabolism changed during the course of HSV infection and that modulating glucose levels can influence the outcome of infection, being detrimental or beneficial according to the stage of viral pathogenesis.

Introduction

Virus infections cause tissue damage in several ways one of which is to induce an inflammatory reaction orchestrated by T cells that respond to viral antigens. One such example is the blinding immuno-inflammatory reaction called stromal keratitis (SK), which occurs in the cornea of the eye following infection with herpes simplex virus (HSV) (1, 2). In such reactions, the pro-inflammatory effector T cells may be more tissue damaging if regulatory components of immunity, such as certain cytokines or cells with regulatory

[#]Corresponding author. Barry T. Rouse: btr@utk.edu.

functions, are deficient (3–6). Thus, one aim of therapy with these usually chronic tissue damaging lesions is to shift the balance of different components involved in the immune response to the infection. Few if any effective therapies are readily available to achieve this objective. However, recent studies in the field of cellular metabolism have drawn attention to the fact that nutrient uptake and their utilization may differ among cell types involved in immune responses (7–9). Moreover, it has become evident that manipulating metabolic pathways represents a potential means of rebalancing immune responses and this approach is being mainly explored in the cancer and autoimmunity fields where the imbalance largely involves different subsets of T cells (10–14).

Application of the metabolic reprogramming approach has focused on manipulating glucose and fatty acid metabolism, which can show major differences between immune cells involved in reactions (15). However, few if any studies so far, have focused on infectious diseases, but this topic is highly relevant since many chronic tissue damaging infections are not subject to control by effective vaccines, or by readily acceptable (or affordable) means of therapy. In fact, targeting metabolic events represents a logical approach to pathogen control since many cause major changes in metabolism not only in cells they infect, but also impact on the function of distant uninfected organs such as the liver, kidney, cardiovascular system and even the brain (16). Some of the general physiological consequences of systemic infections has been highlighted by recent studies (16, 17). However, the general topic of how virus infections, particularly those that cause local infections, influences physiological responses is still poorly understood. Our present studies record some metabolic consequences of local infections in the eye with HSV.

Our results show that ocular HSV infection in mice led to increased fed and fasted blood glucose levels at the time when virus no longer persists in ocular tissues. In addition, CD4 T cells from infected mice showed increased glucose uptake both at the corneal lesion site and in the draining lymph node. The CD4 T cells from HSV infected animals were highly metabolically active and displayed increased glucose uptake in vitro compared to T cells from naïve animals. In vitro experiments also indicated that the effector function of inflammatory T cells was dependent on glucose concentration. Moreover, inhibition of glucose uptake by 2DG limited the differentiation of effector T cells in vitro. In contrast, regulatory T cells (Treg) were unaffected by 2DG in vitro. Finally, and of potential therapeutic relevance, in vivo administration of 2DG resulted in diminished SK lesions, a consequence of reduced effector T cell responses. Taken together, we show that local infection with HSV results in changes in glucose homeostasis causing increased blood glucose levels, which may act to stimulate the generation and sustenance of inflammatory CD4 effector T cells, which, in the special environment of the eye, can result in damaging consequences. Although changes in blood glucose levels were not evident during the acute phase of ocular infection, therapy with 2DG during that phase resulted in death from herpes encephalitis in many animals. Possible explanations for these findings are discussed.

Materials and Methods

Mice and Virus

Female C57BL/6 mice were purchased from Harlan Sprague-Dawley, Inc. (Indianapolis, IN), BALB/c DO11.10 RAG2−/− mice were purchased from Taconic and kept in pathogen free facility where food, water, bedding and instruments were autoclaved. All the animals were housed in American Association of Laboratory Animal Care–approved facilities at the University of Tennessee, Knoxville, Tennessee. All investigations followed guidelines of the Institutional Animal Care and Use Committee, and adhered to the ARVO Statement for the Use of Animals in Ophthalmic and Vision Research. HSV-l RE strain was used in all procedures. Virus was grown in Vero cell monolayers (American Type Culture Collection, Manassas, VA), titrated, and stored in aliquots at −80°C until used.

HSV-1 ocular infection and clinical scoring

Corneal infections of C57BL/6 were conducted under deep anesthesia induced by intra peritoneal (i.p) injection of tribromoethanol (Avertin). Mice were scarified on cornea with a 27-gauge needle, and a 3 μl drop containing 1×10^4 PFU of HSV-1 was applied to the eye. The eyes were examined on different days post infection (dpi) with a slit-lamp biomicroscope (Kowa Company, Nagoya, Japan), and the clinical severity of keratitis of individually scored mice was recorded as previously described (18). Briefly, the scoring system was as follows: 0, normal cornea; +1, mild corneal haze; +2, moderate corneal opacity or scarring; +3, severe corneal opacity but iris visible; +4, opaque cornea and corneal ulcer; +5, corneal rupture and necrotizing keratitis. The naïve-uninfected mice were scarified on cornea with a 27-gauge needle without addition of any virus.

2DG Administration

The 2-deoxy-glucose (2DG) (sigma) was dissolved in PBS and administered intraperitoneally at 500mg/kg twice a day starting from either day 0 or day 5 pi until day 14 after infection. The control group either received an equal volume of PBS or left untreated. The dose of 2DG was based on preliminary dose titrations.

Blood Glucose and cytokine quantification

Blood glucose levels were measured from tail blood at different time point pi using Bayer Contour glucose meter and compared to naïve un-infected animals. For Fasting blood glucose levels animals were fasted for 16 hours in a clean cage with water followed by measurement of glucose levels in the blood from tail. For cytokine measurements, serum was isolated from the blood collected using Retro-orbital bleeding. At least 10 mouse cytokines were profiled using a multiplex platform and data were extracted based on cytokine-specific standards by Eve Technologies (Calgary). Five independent serum samples were used from mice at different time points pi. Serum from control uninfected after 4 days of scarification was used as control.

Flow Cytometric Analysis

At day 15 pi, corneas were excised, pooled group-wise, and digested with liberase (Roche Diagnostics Corporation, Indianapolis, IN) for 45 minutes at 37°C in a humidified atmosphere of 5% CO2. After incubation, the corneas were disrupted by grinding with a syringe plunger on a cell strainer and a single-cell suspension was made in complete RPMI 1640 medium. The single-cell suspensions obtained from corneal samples were stained for different cell surface molecules for fluorescence-activated cell sorting (FACS) analyses. Draining cervical lymph nodes were obtained from mice sacrificed at 15 dpi and single cell suspensions were used. All steps were performed at 4°C. Briefly, cells were stained with respective surface fluorochrome-labeled Abs in FACS buffer for 30 minutes, then stained for intracellular Abs. Finally, the cells were washed three times with FACS buffer and resuspended in 1% paraformaldehyde. The stained samples were acquired with a FACS LSR II (BD Biosciences, San Jose, CA) and the data were analyzed using FlowJo software (Tree Star, Inc., Ashland, OR). To determine the number of IFN-γ producing T cells, intracellular cytokine staining was performed. In brief, corneal cells were either stimulated with PMA (50ng) and Ionomycin (500ng) for 4 hours in the presence of brefeldin A (10 μg/mL) in U-bottom 96-well plates (18). After this period, Live/Dead staining was performed followed by cell surface and intracellular cytokine staining using Foxp3 intracellular staining kit (ebioscience) in accordance with the manufacturer's recommendations. Dead cells were gated out using Live/Dead staining. Cells are mentioned as Th1 if they are CD4+ IFN-γ+ and Treg if they are CD4+ Foxp3+.

For 2-NBDG uptake in vivo, mice were injected i.v. with 100 μg 2-NBDG/mouse diluted in PBS to either naïve C57BL/6 animals or day 15 pi animals. 15 min following the injection cervical DLNs were collected and single cell suspensions were stained as described above and analyzed using flow cytometry (19).

Reagents and antibodies

CD4 (RM4–5), CD45 (53–6.7), CD11b (M1/70), Ly6G (1A8), F4/80 (BM8), IFN-γ (XMG1.2), CD25 (PC61), CD44 (IM7), Foxp3 (FJK-16S), anti-CD3 (145-2C11), anti-CD28 (37.51), GolgiPlug (brefeldin A) and anti-pro-IL-1 beta (NJTEN3) from either ebiosciences or BD biosciences. Anti-Mouse phospho-S6 Ribosomal (D57.2.2E) from Cell signaling and hGlut1 from R&D. Phorbol myristate acetate (PMA) and Ionomycin from sigma. Live/Dead staining kit and 2-NBDG from Life Technologies. Recombinant IL-2, IL-12, IL-6 and TGF-β from R&D systems. Glucose free RPMI media (life technologies) was prepared using dialyzed FBS and glucose (sigma) was added at concentrations (0.1–20mM).

Quantitative PCR (qPCR)

At day 2 post ocular infection with HSV-1, the corneas were isolated and two corneas were pooled per sample/group. Naïve CD4 T cells or cells activated in vitro with or without 2DG were taken at least 100,000 cells/sample. Total RNA from corneal and isolated T cell populations was isolated using mirVana miRNA isolation kit (Ambion). Liver (≤30mg) was isolated at day 0, day 4, day 8 and day 15 pi and total RNA was extracted using RNeasy® Fibrous Tissue Mini Kit (Qiagen) as per manufacturer's recommendation. cDNA was made with 500ng of RNA (corneal samples) and entire RNA (isolated T cells) by using oligo(dT)

primer and ImProm-II Reverse Transcription system (Promega). Taqman gene expression assays for Glut-1 (SLC2A1), HK1 (Hexokinase 1), HK2 (Hexokinase 2), Il6ra, Tnfrsf1b, Stat3, Ifngr1, Cyp7a1, Rhoc, Il1a, Ifnb, Tnfa and Il1b were purchased from Applied biosystems and quantified using 7500 Fast Real-Time PCR system (Applied Biosystems). The expression levels of different molecules were normalized to β-actin using ΔCt calculation. Relative expression between control and experimental groups was calculated using the $2^{-\Delta\Delta Ct} \times 1000$ formula.

Purification of CD4+ T cells

CD4+ T cells (total or naïve) were purified from single cell suspension of pooled draining cervical lymph nodes (DLNs) and spleen from HSV-infected or naïve C57BL/6 mice using a mouse total or naïve CD4+ T cell isolation kit according to the manufacturer's instructions (Miltenyi Biotec, Auburn, CA). The purity was achieved at least to an extent of 95%.

In vitro Treg and Th1 differentiation

For glycolysis measurements using seahorse extracellular flux analyzer, naïve CD4 T cells were used in Treg and Th1 differentiation. For experiments evaluating the effects of glucose concentrations or effects of 2DG, splenocytes from naïve DO11.10 RAG2 −/− mice were used as a precursor population for the induction of Treg and Th1 cells as previously described (18). Briefly, 1×10^6 splenocytes after RBC lysis and several washings or 1 million naïve CD4 T cells were cultured in 1ml glucose sufficient RPMI media or glucose free-RPMI media (dialyzed serum) containing rIL-2 (100 U/ml) and TGFβ (1–5ng/ml) in the presence or absence of various concentrations of Glucose (0.5–20mM) with plate bound anti-CD3/CD28 Ab (1 μg/ml) for 5 days at 37°C in a 5% CO2 incubator. After 5 days, samples were characterized for Foxp3 intracellular staining (ebioscience staining kit) analyzed by flow cytometry. For Th1 differentiation, cells were cultured in the presence of recombinant mouse IL-12 (5–10ng/ml) and anti-IL-4 (10 μg/ml). After 5-days samples were re-stimulated with PMA/Ionomycin and analyzed for the production of IFN-γ by intracellular cytokine staining kit (BD biosciences) using flow cytometer. 250μM-2DG dose was chosen based on the preliminary dose response experiments and previous reports (20).

OCR and ECAR measurement

OCR and ECAR values were measured using a Seahorse XF24 metabolic analyzer. Briefly, total CD4 T cells were purified from either infected or naïve female B6 mice or Treg/Th1 cells were differentiated and expanded from naïve CD4 T cells in vitro as described above. 1×10^6 cells per well were plated on XF24 plate (Seahorse Bioscience) pre-coated with 0.5 mg/ml poly-D lysine (Sigma). Cells were maintained in RPMI media (corning) supplemented with 1mM sodium pyruvate (Sigma) and 10% FBS. Before analyzing, cells were spun down and 530ul of XF media (with or without glucose) was added to each well, followed by incubation for 30 minutes in CO2-free incubator at 37°C. Seahorse analyzer was then run per manufacture's protocol with oligomycin (1uM), FCCP (1uM), and antimycin A (1uM) injected through ports A, B, and C respectively for mitochondrial stress test and glucose (10mM), oligomycin (1uM) and 2DG(10mM) for glycolysis stress test (21).

Viral Plaque Assay

Virus titers were measured in the brain and corneas of HSV infected mice as described previously by others (22). Virus titers in all samples were measured using standard plaque assay as described previously (22, 23).

Cell Culture

Female C57BL/6 mice were used at 8–16 weeks of age. BMDMs were generated as described previously (24) and grown in RPMI 1640 with 10% FCS. The media was supplemented with macrophage-colony-stimulating factor (10 ng/ml). Cells were 98% pure for macrophages (CD45+ CD11b+ F4/80+) and plated out on day 10 at 100,000 cells/well and stimulated with LPS (20ng/ml) for 24 hours.

Statistical Analysis

Statistical significance was determined by either Student's t-test (comparing two groups) or One-way ANOVA (comparing three or more groups). A P-value of <0.05 was regarded as a significant difference between groups: *P ≤ 0.05, **P ≤ 0.01, ***P ≤ 0.001. GraphPad Prism software (GraphPad Software, Inc., La Jolla, CA) was used for statistical analysis.

Results

HSV-1 infection increases blood glucose levels

To ascertain if ocular infection with HSV led to changes in glucose metabolism, blood glucose levels were measured in control and infected animals up to 15 days post infection (pi), the time when inflammatory responses to the ocular infection were at their peak. Elevated blood glucose levels were not observed in the initial period after infection when replicating virus was present in the eye. However, a moderate increase (about 1.5 to 2 fold) in blood glucose levels occurred in samples from days 8, a time when ocular inflammatory lesions first become evident in the corneal stroma, as well as at day 15 pi (Fig. 1A). However, at the latter time point the effect was more variable and differences were not significant in some experiments. At day 15, comparisons of blood glucose levels were also made between infected and uninfected animals following a 16-hour fasting period. Once again glucose levels were significantly higher ($p<0.01$) in the infected animals compared to uninfected controls in both the fed and fasting states. (Fig. 1B).

Previous studies indicated that low-grade inflammation can affect systemic glucose levels by inducing gene expression changes in the liver (25, 26). Accordingly, pro-inflammatory cytokine levels in the serum were measured at different time points pi. The results indicated that IL-6, TNF-α and IFN-γ cytokine levels were significantly increased in serum samples of day 4 pi animals compared to uninfected controls (Fig. 1C). Measurement of gene expression changes in the liver at different time points pi indicated a significant increase in the expression of genes in the signaling pathways of pro-inflammatory cytokines at day 8 pi (about 3 fold) which included Il6ra, Tnfr2, Ifnγr1 and Stat3 (Fig. 1D). A recent report suggests that systemic inflammation suppressed CYP7A1 (Cholesterol 7 alpha-hydroxylase), the rate-limiting enzyme of the bile acid biosynthesis in the liver (25). This led to the accumulation of intermediate metabolites of the mevalonate pathway, resulting in

stabilization of RHOC, a small GTPase induced by inflammation. The outcome was fasting hyperglycemia. We also quantified the expression of both CYP7A1 and RHOC in the liver at day 8 pi the time when blood glucose was at its peak. While the expression of CYP7A1 was significantly reduced, the expression of RHOC was higher in the livers at day 8 pi (Fig. 1E). These data indicate that ocular infection with HSV-1 results in a change in glucose metabolism likely by effects on the liver mediated by responses to inflammatory cytokines.

CD4 T cells display enhanced glucose uptake and glycolysis

As the inflammatory response in the eye to HSV infection is mainly orchestrated by CD4+ T cells (1), changes in glucose uptake and glycolytic events was measured in CD4 T cells of animals with SK lesions and compared to CD4 T cells in uninfected animals. The first series of experiments compared glucose uptake in control uninfected and animals with lesions (day 15 pi), following the administration of a fluorescently labeled glucose analog 2-NBDG (2-(N-(7-Nitrobenz-2-oxa-1,3-diazol-4-yl) Amino)-2-Deoxyglucose). One hour later, the draining lymph nodes (DLN) were collected and the fraction of CD4+ T cells that took up 2-NBDG was measured by flow cytometry. The results indicated that the CD4+ T cells from mice with ocular lesions had significantly more cells (approximately 6-fold) that took up the glucose compared to uninfected controls (Fig. 2A, B). Of note, compared to uninfected animals, CD4+ T cells from infected mice contained 4-fold more cells with the effector memory phenotype and 7-fold more cells that produced IFN-γ when stimulated *in vitro* with PMA and Ionomycin (Supp. Fig. 1). The glucose uptake receptor GLUT1, as measured by flow cytometry was also increased in CD4 T cells at day 15 pi compared to cells from uninfected controls (Fig. 2C).

Given that the CD4+ T cells from infected animals exhibited enhanced glucose uptake, a second set of experiments measured if these CD4+ cells also had changes in glucose metabolism. This was done using seahorse technology by determining the extracellular acidification rate (ECAR), which serves as an indicator of lactate production and glycolytic activity (21). CD4+ T cells isolated from the DLN of infected animals (day 15 pi) had a higher basal and maximal glycolytic rate (>3-fold) compared to CD4+ T cells from uninfected animals (Fig. 2D). Of note, measurements of basal oxygen consumption rate (OCR), which serves as an indicator mitochondrial respiration (21), indicated that the ratio of OCR to ECAR was significantly reduced ($p<0.05$) in cells from infected animals. This result may indicate cellular preference for glycolysis over mitochondrial respiration (Fig. 2E). These results imply that upon infection with HSV-1, CD4+ T cells increase glucose uptake and glucose utilization (glycolysis), which might be supported by higher glucose levels observed in animals with inflammatory lesions.

Treg and effector cells differentially use glucose

Since different T cell subsets participate in SK reactions (1), it was of interest to determine the type of T cell subset in which changes in glucose metabolism was occurring. The focus was on CD4 effector and regulatory T cells since these are the two major subsets which influence the extent of SK lesions (3, 4). The two cell types were isolated from the DLN of day 15 infected mice, separating them based on their expression levels of the IL-2 receptor CD25 with cells that were CD25+ taken to be mainly Treg. Thus in separate experiments,

we could show that on average ~93% of the CD25+ T cells were Foxp3+ on day 15 pi, The CD4+CD25− population was considered to be predominantly effector T cells (Supp. Fig. 2). The uptake of 2NBDG was significantly higher in the CD25− population (mainly effector T cells) as compared to the CD25+ population (mainly Treg) (Fig 3A).

Since, the mTOR pathway is also involved in the control of glucose uptake and glycolysis in T cells (27), mTOR activity was compared in the two subsets. This was done by measuring the phosphorylation of S6 kinase (a component of the mTOR down-stream signaling cascade) (28). Higher glucose uptake in the CD25− CD4 effector population was also associated with higher mTOR activity compared to the activity of the CD25+ CD4 Treg population (Fig. 3B).

To further determine if glucose requirements differed between the Th1 effector and Treg subsets, experiments were done in vitro to generate Treg and Th1 populations from naïve DLN populations. The populations obtained were approximately 80% enriched for each subset. After 5 days, levels of glycolysis were compared in the two populations by using a glycolysis stress test which measures extracellular flux analysis (ECAR). As shown in Fig 3C, the basal ECAR levels were elevated in the Th1 population compared to the Treg population (2.8-fold). In addition, the glycolytic capacity, as measured by an increase in ECAR levels following inhibition of ATP synthase (using oligomycin) (21), was around 3 fold higher in Th1 compared to the Treg cells (Fig. 3C). Accordingly, the two major populations of CD4 T cells involved in SK lesions had distinct differences in glucose metabolism, a pattern of events noted in some autoimmune and neoplastic diseases (11, 13).

Glucose availability affects Th1 differentiation in vitro

To begin to approach the question of the potential relevance of raised glucose levels during the inflammatory response to HSV infection, in vitro experiments were done to measure the influence of glucose levels on the efficiency of Th1 and Treg cell differentiation, cell types critically involved in SK reaction (1, 4). For this naïve CD4 T cells were TCR stimulated under either Treg or Th1 inducing conditions after which the effect of supplementing cultures with different concentrations of glucose was measured. Levels of glucose evaluated varied from below physiological levels to hyperglycemic (0.5mM to 20mM). As shown in the Fig 4A, B, increasing glucose levels elevated the magnitude of Th1 responses, but had no significant influence on Treg responses, as noted previously (29, 30). Curiously, increasing glucose from physiological levels (about 5mM) to that observed in vivo in the infected mice at day 8 pi (maximum of 10mM) led to a significant increase ($P<0.05$) in Th1 differentiation. (Fig. 4C). The above observation supports the hypothesis that, a two-fold increase in the physiological levels of glucose in the periphery might be relevant in terms of enhancing the generation of Th1 cells in vivo.

Inhibition of glucose utilization using 2-deoxyglusose inhibits the glycolysis

To further measure the influence of glucose levels during the inflammatory response to HSV infection, experiments were done in vitro to measure the effect of the molecule 2DG, which inhibits glucose utilization and hence glycolysis. Naïve CD4 T cells were activated in the presence of 2DG for 72 hours followed by measurement of basal glycolysis using

extracellular flux analysis The data indicated a 3-fold reduction in basal ECAR levels indicating a decrease in basal glycolysis in cells activated in the presence of 2DG when compared to control activated cells (Fig. 5A). Of note, no difference in cell death was observed at the concentration of 2DG used (data not shown). Collectively, the above results support the hypothesis that activated T cells upregulate glycolysis which can be inhibited by 2DG.

Additional experiments were done to measure the expression of key genes involved in the glycolytic pathway both in the presence or absence of 2DG. Naïve CD4 T cells were activated in vitro by stimulating them with anti-CD3/CD28 for 24 hours and the effect of 2DG (250μM) on gene expression changes was recorded. Compared to naïve CD4 T cells, activated CD4 T cells expressed higher levels of several genes involved in glycolysis. These included Hexokinase-1 (2-fold), Hexokinase-2 (20-fold) and Glut1 (4-fold) (Fig. 5). However, when CD4 T cells were activated in the presence of 2DG, the genes involved in glycolysis remained at the levels or even below those observed in non-activated control cells. (Fig. 5B). The presence of 2DG in the cultures also served to switch off the raised mTOR activity, as measured by levels of phosphorylated S6 kinase using flow cytometry (Fig. 5C).

To measure the effect of inhibition of glycolysis on differentiation of the two CD4 T cell subsets of interest (Th1 and Treg), naïve CD4+ T cells were cultured in Treg or Th1 differentiating conditions for 5 days in the presence or absence of 2DG (250μM). Although, the differentiation of Treg was unaffected at the dose of 2DG used, a 20-fold reduction in the numbers of Th1 cells induced was observed in the presence of 2DG (Fig. 6). These results support the above findings that effector T cell use glycolysis to a higher extent than Treg. The results may also mean that 2DG therapy could be therapeutically useful against SK by inhibiting T effectors but leaving Treg function intact. This notion is tested in the next section.

Inhibition of glucose utilization limits SK lesion severity and diminishes effector T cell responses

To measure the therapeutic potential of 2DG against SK, HSV infected animals were given daily administrations of either 2DG or PBS (control) starting at day 5 pi. This is the time point when there is at best minimal replicating virus detectable in the infected corneas and early inflammatory reactions start to become evident. Animals were examined at day 15 pi to record and compare the severity of SK lesions. The results were clear cut with animals receiving 2DG therapy showing significantly reduced SK lesion severity ($P<0.01$) compared to PBS treated control animals (Fig. 7A). At day 15 pi, around 12% of 2DG treated animals showed a lesion score of ≥ 3.0 compared to 50% in control treated animals. At the termination of experiments on day 15 pi, pools of corneas were collected and processed to identify their cellular composition by FACS analysis. There was a reduction in the number of total CD4 T cells (~10 fold) infiltrating the corneas of 2DG treated animals compared to control animals (Fig. 7B).

In parallel experiments of similar design, pools of corneas, DLN and spleen were collected at 15 days pi from 2DG treated and control animals. Single cell suspensions were stimulated in vitro with PMA and ionomycin to activate T cells and to record the numbers of cells that

were either IFN-γ producers or expressed the transcription factor Foxp3. In the corneas, the number of CD4 T cells expressing IFN-γ was reduced approximately 8-fold in 2DG compared to untreated controls (Fig. 7C). In the DLN and spleen, 2DG treatment resulted in reduced frequency and numbers of IFN-γ producing CD4 T cells by about 2-fold. Although the frequency of Tregs in the DLN remained the same, their number decreased significantly. This might be explained by reduced inflammatory responses in treated animals. However, the number and frequency of Treg in the spleens of 2DG treated animals remained unchanged (Fig. 7D).

Taken together, our results indicate that daily administration of 2DG starting at day 5 pi significantly diminished HSV-1 induced immunopathology along with a reduction in effector T cell numbers in both the cornea and lymphoid organs, which could in part contribute to reduced lesion severity.

Inhibiting of glucose utilization is lethal in the acute phase of HSV infection

Although, we found no evidence for hyperglycemia in the acute phase of HSV infection, experiments were done to measure the effects of 2DG therapy at the time when virus was actively replicating in the infected cornea. Animals were ocularly infected with HSV-1 and were either treated daily with 2DG or PBS control, starting from the day of infection. Under the infection conditions used, HSV infection of untreated animals failed to cause detectable illness or signs of encephalitis. However, in the 2DG treated animals around 40–50% (in three separate experiments) of 2DG treated animals developed encephalitis and most had to be terminated by day 10 pi (Fig. 8A). By 8 days pi, affected animals became lethargic, lost weight, showed ruffled fur and hunched appearance along with signs of incoordination. Brains were collected from encephalitic 2DG treated animals, to quantify levels of virus present. High virus levels of HSV were detectable (>4 log) in brain homogenates in all animals that showed signs of encephalitis by day 10 pi (Fig. 8B). These animals also had detectable virus in ocular swabs at day 6 pi which is one day beyond the time when virus is regularly present in untreated infected animals. Additionally, levels of virus in ocular swabs were around tenfold higher than in untreated mice (Fig. 8C). Of note, virus could not be detected in the brains at day 10 pi or in the ocular tissue at day 6 pi in the control animals when infected with the same dose of virus that caused encephalitis in the 2DG treated animals.

The reduction in antiviral inflammatory cells or mediators could explain the increased viral burden in the animals treated with 2DG. To test this possibility, pools of corneas were isolated from animals treated with 2DG or PBS controls at day 2 pi and were evaluated for the abundance of macrophages and neutrophils. In addition, the effector function of macrophages and neutrophils was measured by the expression of pro-IL-1β using flow cytometry. While the number and frequency of pro-IL-1beta expressing neutrophils remained unchanged with 2DG treatment (Supp. Fig 3), the frequency and the number of pro-IL-1beta expressing macrophages in the cornea were significantly reduced in 2DG treated animals (>3-fold) (Fig. 8D). This might account for the failure to stop the spread of virus to the CNS. To assess if molecules involved in antiviral responses were affected upon 2DG treatment, the expression of IFN-β, IL-1α and TNF-α genes was determined in the

corneas of both control and 2DG treated animals at day 2pi. The results indicated no significant differences in the expression of these molecules (Fig. 8E). Taken together, the increase in viral load in the cornea as well as the failure to stop the spread of virus to the brain could be in part explained by reduction in the innate effector function of macrophages which also require glucose for their function as demonstrated in the next section.

2DG reduces the macrophage activation in the presence of LPS

Macrophages are reported to play an important role in early stages of infection by controlling HSV-1 replication and dissemination within the TG (31). Hence, effects of 2DG on macrophage activation were measured using LPS stimulation of bone marrow derived macrophages (BMDM). BMDM's were stimulated with LPS in the presence or absence of 2DG (250μM) for 24 hours, followed by measurement of pro-IL-1β expression using flow cytometry. The results indicated that stimulation of macrophages with LPS in the presence of 2DG resulted in a 2-fold reduction in both the frequency of macrophages expressing pro-IL-1β and expression of pro-IL-1β per cell basis (MFI) as compared to LPS stimulation alone (Fig. 8F), supporting the previous reports (32). In conclusion, inhibition of glucose utilization in macrophages inhibited the effector function of macrophages, which might partially explain the high viral burden in the animals treated with 2DG.

Discussion

Inflammatory reactions are likely to be prolonged and cause excessive tissue damage when the activity of the principal orchestrators, usually either CD4 or CD8 T cells, are not constrained by inhibitory molecules or by cells that function as regulators (3–6). This is the state of affairs in the viral infection model we have used in this report wherein CD4 T cell driven inflammatory reactions in the eye cause a chronic vision-impairing lesion called stromal keratitis. The challenge with SK is to understand the events that result in lesions and to find therapies that limit the severity and duration of ocular damage. In the present report, we make the unexpected finding that blood glucose levels change significantly during the course of infection. Whereas levels remained normal during the early phase of infection when the virus was actively replicating in the cornea, they increased around two fold during the time when inflammatory responses to the virus was occurring. We could show that glucose levels influenced the extent of induction of the inflammatory T cell subset in vitro that mainly drives SK lesions, but not regulatory T cells. Additionally, if glucose utilization was limited in vivo as a consequence of therapy in the inflammatory phase with the drug 2DG, lesions were diminished compared to untreated infected controls. In addition, lesions in 2DG treated animals contained less pro-inflammatory effectors. Glucose metabolism also influenced the acute phase of infection when replicating virus was present in the eye. Thus, therapy with 2DG to limit glucose utilization caused mice to become susceptible to the lethal effects of HSV infection, with virus spreading to the brain causing encephalitis. Taken together, our results indicate that glucose metabolism changed during the course of HSV infection and that modulating glucose levels can influence the outcome of infection, being detrimental or beneficial according to the stage of viral pathogenesis.

Few reports have noted any changes in blood glucose levels in response to virus infections except in experimental situations where infection can set off diabetes mellitus (33, 34). Moreover, in the situation we described the mild hyperglycemia was absent during the time when virus was actively replicating in the eye or elsewhere in the body. Instead, the hyperglycemia only occurred during the inflammatory reaction to the virus, which in the case of HSV ocular infection becomes a vision-impairing lesion referred to as stromal keratitis. Moreover, SK is a local lesion in the eye accompanied by an inflammatory response in the innervating trigeminal ganglion (35). Two relevant questions emerge. These are, what accounts for the mild hyperglycemia and does the event have any consequence.

With regard to causation, the likeliest explanation could be the production of factors from the inflammatory site that caused the liver to change its level of glucose production. Candidates could include hormones, cytokines, or the release of lipid mediators from inflammatory cells (36–39). In a complex model of sustained inflammation induced by LPS, elevated blood glucose levels were observed and these were shown to be mediated by TNF-α (25). This cytokine acted on the liver to suppress the expression of the bile acid biosynthesis enzyme CYP7A1 that normally functions to influence glucose production by acting on the hepatic mevalonate pathway, resulting in the inhibition of insulin signaling (25). In our system, components of the virus with Toll-like receptor components would likely not be involved since virus is absent in the blood stream especially at the time of raised glucose levels. However, we did observe increased blood levels of some cytokines, which included TNF-α, IL-6 and IFN-γ at day 4 pi, as well as an increase in the expression of their receptors in the liver at day 8 pi. Moreover, we could show that animals with high blood glucose levels had reduced levels of CYP7A1, which could mean that the mechanism inducing the hyperglycemia was similar to that described by the Medzhitov group (25). Additional experiments are underway to further evaluate potential mechanisms that could cause raised glucose levels in our system, which differs from the systemic model used by the Medzhitov group (25) in being only a local inflammatory lesion in a small organ, the eye.

The second question about the hyperglycemia observed was the issue of its potential relevance. Two lines of indirect evidence implied that the effect could have relevance. Firstly, the change of glucose levels was about two-fold and whether this change in glucose concentration was potentially meaningful was tested in an in vitro induction system. In this system, the levels of CD4 Th1 effector cells generated from naïve precursors were compared using media with controlled concentrations of glucose. Curiously increasing the glucose concentrations from physiological levels to the levels observed in infected animals significantly increased the number of effector Th1 cells induced and had no effect on the levels of Treg induction, confirming the previous observations (29, 30). This could mean that the 2-fold increase in blood glucose observed in vivo might also serve to enhance Th1 differentiation, but further studies are needed to verify this possibility.

Another indirect approach also indicated that the change in glucose levels might help drive the inflammatory T cell response. Accordingly, when glucose utilization was suppressed by treating mice with 2DG from the time of onset of ocular inflammation, SK lesions were significantly reduced in magnitude. Along with this, the composition of the cellular constituents involved in ocular lesions was markedly changed with reduced numbers of CD4

effectors. Other reports have also shown that 2DG therapy (13, 14) can control both auto-inflammatory lesions and GVHD inflammatory reactions. However, in these inflammatory models, therapy with 2DG alone was usually non-effective and additional antimetabolite therapies such as metformin (13) and 6-Diazo-5-oxo-L-norleucine - DON (14) were needed to be used in combination to counteract lesions. The fact that 2DG alone was highly effective therapy against SK, could relate to the less chronic nature of the SK lesion since viral antigen does not persist to drive lesions. However, in the autoimmune disease and GvHD system the inflammatory cells in the lesions are under consistent activation.

One issue yet to be explained was the discrepancy with the dose of 2DG used to achieve therapeutic effects in vivo with that found to selectively inhibit inflammatory T cell responses in vitro. However, we could not measure the absolute concentrations of 2DG in the blood and DLN after in vivo administration, and it is well known that 2DG is rapidly metabolized in vivo (40). Another perplexing issue was the observation that 2DG could inhibit the effects of glucose in vitro when the later was far in excess of 2DG concentrations. Some data from studies with yeast at least partially explain such observations. Thus 2DG may inhibit the function of glucose transporters (41) and it is conceivable that 2DG has additional off target effects not mediated by glucose itself (42). These issues needs to be further clarified.

Another unexpected observation made in this report was the dramatic consequence of 2DG therapy administered during the acute phase of ocular HSV infection. In such experiments, many of the animals succumbed to lethal consequences with virus spreading to and replicating in the CNS. Herpetic encephalitis (HSE) is a very rare outcome of HSV infections in adult humans unless they are genetically compromised in some immune component (43–46). In animal models for HSV infection, HSE is a more common event and can occur at higher doses of infection, or with some virulent strains of virus, or if animals have one of several defects of either innate or adaptive immunity (22, 47–50). We strongly suspect that the lethal consequences of HSV infection in 2DG treated mice could be the result of impaired function of a protective component of innate immunity. So far we have minimal support for this idea, but could show that the number of IL-1β expressing macrophages but not neutrophils was reduced at the site of infection as a consequence of 2DG therapy. In addition, that animals can suffer lethal consequences when treated with 2DG as was noted with another viral model (16). Accordingly, with influenza, the lethal effects were attributed to the increased expression of the ER-stress-induced transcription factor CHOP protein and its target gene Gadd34 in the hindbrains of mice treated with 2DG. The increased expression of CHOP protein caused apoptosis of neurons leading to neuronal dysfunction and death. This phenomenon has yet to be evaluated in our HSE model, but we suspect to find differences since HSV replication occurs in the CNS and can be very destructive resulting from both direct viral and immune-pathological destructive events (22, 48, 49).

This study is one of the first to evaluate the use of a drug which influences metabolic processes used by different immune components responding to an infection. We show that modulating the main energy generating component of inflammatory T cells has value to modulate the extent of viral immune inflammatory lesions. In our system, the effect was

particularly effective since 2DG therapy inhibited pro-inflammatory T effectors but had no direct effect on cells such as Treg that play a protective function in SK lesions. Our results also indicate that using metabolic modifying drugs should be used with caution especially during virus infections. Thus when 2DG therapy was used when the virus was still replicating, the viral replication was enhanced and this could have had lethal consequences as a result of virus spreading to the brain.

Supplementary Material

Refer to Web version on PubMed Central for supplementary material.

Acknowledgments

This study was supported by National Institutes of Health Grant EY 005093

References

1. Biswas PS, Rouse BT. Early events in HSV keratitis—setting the stage for a blinding disease. Microbes and Infection. 2005; 7:799–810. [PubMed: 15857807]
2. Rowe A, Leger AS, Jeon S, Dhaliwal D, Knickelbein J, Hendricks R. Herpes keratitis. Progress in retinal and eye research. 2013; 32:88–101. [PubMed: 22944008]
3. Veiga-Parga T, Sehrawat S, Rouse BT. Role of regulatory T cells during virus infection. Immunological reviews. 2013; 255:182–196. [PubMed: 23947355]
4. Suvas S, Azkur AK, Kim BS, Kumaraguru U, Rouse BT. CD4+ CD25+ regulatory T cells control the severity of viral immunoinflammatory lesions. The Journal of Immunology. 2004; 172:4123–4132. [PubMed: 15034024]
5. Sarangi PP, Sehrawat S, Suvas S, Rouse BT. IL-10 and natural regulatory T cells: two independent anti-inflammatory mechanisms in herpes simplex virus-induced ocular immunopathology. The Journal of Immunology. 2008; 180:6297–6306. [PubMed: 18424753]
6. Tumpey TM, Elner VM, Chen S-H, Oakes JE, Lausch RN. Interleukin-10 treatment can suppress stromal keratitis induced by herpes simplex virus type 1. The Journal of Immunology. 1994; 153:2258–2265. [PubMed: 8051423]
7. O'Sullivan D, Pearce EL. Targeting T cell metabolism for therapy. Trends in immunology. 2015; 36:71–80. [PubMed: 25601541]
8. O'Neill LA, Kishton RJ, Rathmell J. A guide to immunometabolism for immunologists. Nature Reviews Immunology. 2016
9. MacIver NJ, Michalek RD, Rathmell JC. Metabolic regulation of T lymphocytes. Annual review of immunology. 2013; 31:259–283.
10. Pearce EL, Walsh MC, Cejas PJ, Harms GM, Shen H, Wang L-S, Jones RG, Choi Y. Enhancing CD8 T-cell memory by modulating fatty acid metabolism. Nature. 2009; 460:103–107. [PubMed: 19494812]
11. Chang C-H, Curtis JD, Maggi LB, Faubert B, Villarino AV, O'Sullivan D, Huang SC-C, van der Windt GJ, Blagih J, Qiu J. Posttranscriptional control of T cell effector function by aerobic glycolysis. Cell. 2013; 153:1239–1251. [PubMed: 23746840]
12. Chang C-H, Qiu J, O'Sullivan D, Buck MD, Noguchi T, Curtis JD, Chen Q, Gindin M, Gubin MM, van der Windt GJ. Metabolic competition in the tumor microenvironment is a driver of cancer progression. Cell. 2015; 162:1229–1241. [PubMed: 26321679]
13. Yin Y, Choi S-C, Xu Z, Perry DJ, Seay H, Croker BP, Sobel ES, Brusko TM, Morel L. Normalization of CD4+ T cell metabolism reverses lupus. Science translational medicine. 2015; 7:274ra218–274ra218.

14. Lee C-F, Lo Y-C, Cheng C-H, Furtmüller GJ, Oh B, Andrade-Oliveira V, Thomas AG, Bowman CE, Slusher BS, Wolfgang MJ. Preventing allograft rejection by targeting immune metabolism. Cell reports. 2015; 13:760–770. [PubMed: 26489460]
15. Gerriets VA, Rathmell JC. Metabolic pathways in T cell fate and function. Trends in immunology. 2012; 33:168–173. [PubMed: 22342741]
16. Wang A, Huen SC, Luan HH, Yu S, Zhang C, Gallezot J-D, Booth CJ, Medzhitov R. Opposing effects of fasting metabolism on tissue tolerance in bacterial and viral inflammation. Cell. 2016; 166:1512–1525. e1512. [PubMed: 27610573]
17. Rao S, Schieber AMP, O'Connor CP, Leblanc M, Michel D, Ayres JS. Pathogen-Mediated Inhibition of Anorexia Promotes Host Survival and Transmission. Cell. 2017; 168:503–516. e512. [PubMed: 28129542]
18. Varanasi SK, Reddy PB, Bhela S, Jaggi U, Gimenez F, Rouse BT. Azacytidine treatment inhibits the progression of Herpes Stromal Keratitis by enhancing regulatory T cell function. Journal of Virology. 2017; 91:e02367–02316. [PubMed: 28100624]
19. O'Sullivan D, van der Windt GJ, Huang SC-C, Curtis JD, Chang C-H, Buck MD, Qiu J, Smith AM, Lam WY, DiPlato LM. Memory CD8+ T cells use cell-intrinsic lipolysis to support the metabolic programming necessary for development. Immunity. 2014; 41:75–88. [PubMed: 25001241]
20. Gerriets VA, Kishton RJ, Nichols AG, Macintyre AN, Inoue M, Ilkayeva O, Winter PS, Liu X, Priyadharshini B, Slawinska ME. Metabolic programming and PDHK1 control CD4+ T cell subsets and inflammation. The Journal of clinical investigation. 2015; 125:194–207. [PubMed: 25437876]
21. van der Windt GJ, Chang CH, Pearce EL. Measuring Bioenergetics in T Cells Using a Seahorse Extracellular Flux Analyzer. Current Protocols in Immunology. 2016:3.16 B. 11–13.16 B. 14.
22. Bhela S, Mulik S, Reddy PB, Richardson RL, Gimenez F, Rajasagi NK, Veiga-Parga T, Osmand AP, Rouse BT. Critical role of microRNA-155 in herpes simplex encephalitis. The Journal of Immunology. 2014; 192:2734–2743. [PubMed: 24516198]
23. Reddy PB, Sehrawat S, Suryawanshi A, Rajasagi NK, Mulik S, Hirashima M, Rouse BT. Influence of galectin-9/Tim-3 interaction on herpes simplex virus-1 latency. The Journal of Immunology. 2011; 187:5745–5755. [PubMed: 22021615]
24. Gonçalves R, Mosser DM. The isolation and characterization of murine macrophages. Current protocols in immunology. 2008:14.11. 11–14.11. 16.
25. Okin D, Medzhitov R. The effect of sustained inflammation on hepatic mevalonate pathway results in hyperglycemia. Cell. 2016; 165:343–356. [PubMed: 26997483]
26. Masri S, Papagiannakopoulos T, Kinouchi K, Liu Y, Cervantes M, Baldi P, Jacks T, Sassone-Corsi P. Lung adenocarcinoma distally rewires hepatic circadian homeostasis. Cell. 2016; 165:896–909. [PubMed: 27153497]
27. Ray JP, Staron MM, Shyer JA, Ho P-C, Marshall HD, Gray SM, Laidlaw BJ, Araki K, Ahmed R, Kaech SM. The interleukin-2-mTORc1 kinase axis defines the signaling, differentiation, and metabolism of T helper 1 and follicular B helper T cells. Immunity. 2015; 43:690–702. [PubMed: 26410627]
28. Nojima H, Tokunaga C, Eguchi S, Oshiro N, Hidayat S, Yoshino K-i, Hara K, Tanaka N, Avruch J, Yonezawa K. The mammalian target of rapamycin (mTOR) partner, raptor, binds the mTOR substrates p70 S6 kinase and 4E–BP1 through their TOR signaling (TOS) motif. Journal of Biological Chemistry. 2003; 278:15461–15464. [PubMed: 12604610]
29. Cham CM, Gajewski TF. Glucose availability regulates IFN-γ production and p70S6 kinase activation in CD8+ effector T cells. The Journal of Immunology. 2005; 174:4670–4677. [PubMed: 15814691]
30. Michalek RD, Gerriets VA, Jacobs SR, Macintyre AN, MacIver NJ, Mason EF, Sullivan SA, Nichols AG, Rathmell JC. Cutting edge: distinct glycolytic and lipid oxidative metabolic programs are essential for effector and regulatory CD4+ T cell subsets. The Journal of Immunology. 2011; 186:3299–3303. [PubMed: 21317389]

31. Kodukula P, Liu T, Van Rooijen N, Jager MJ, Hendricks RL. Macrophage control of herpes simplex virus type 1 replication in the peripheral nervous system. The Journal of Immunology. 1999; 162:2895–2905. [PubMed: 10072539]
32. Tannahill G, Curtis A, Adamik J, Palsson-McDermott E, McGettrick A, Goel G, Frezza C, Bernard N, Kelly B, Foley N. Succinate is an inflammatory signal that induces IL-1 [bgr] through HIF-1 [agr]. Nature. 2013; 496:238–242. [PubMed: 23535595]
33. Filippi CM, von Herrath MG. Viral trigger for type 1 diabetes. Diabetes. 2008; 57:2863–2871. [PubMed: 18971433]
34. Coppieters KT, Boettler T, von Herrath M. Virus infections in type 1 diabetes. Cold Spring Harbor perspectives in medicine. 2012; 2:a007682. [PubMed: 22315719]
35. Khanna KM, Lepisto AJ, Decman V, Hendricks RL. Immune control of herpes simplex virus during latency. Current opinion in immunology. 2004; 16:463–469. [PubMed: 15245740]
36. Chen L, Chen R, Wang H, Liang F. Mechanisms linking inflammation to insulin resistance. International journal of endocrinology. 2015
37. Glass CK, Olefsky JM. Inflammation and lipid signaling in the etiology of insulin resistance. Cell metabolism. 2012; 15:635–645. [PubMed: 22560216]
38. Shoelson SE, Lee J, Goldfine AB. Inflammation and insulin resistance. The Journal of clinical investigation. 2006; 116:1793–1801. [PubMed: 16823477]
39. McGuinness OP. Defective glucose homeostasis during infection. Annu. Rev. Nutr. 2005; 25:9–35. [PubMed: 16011457]
40. Gounder MK, Lin H, Stein M, Goodin S, Bertino JR, Kong ANT, DiPaola RS. A validated bioanalytical HPLC method for pharmacokinetic evaluation of 2-deoxyglucose in human plasma. Biomedical Chromatography. 2012; 26:650–654. [PubMed: 21932382]
41. O'Donnell AF, McCartney RR, Chandrashekarappa DG, Zhang BB, Thorner J, Schmidt MC. 2-Deoxyglucose impairs Saccharomyces cerevisiae growth by stimulating Snf1-regulated and α-arrestin-mediated trafficking of hexose transporters 1 and 3. Molecular and cellular biology. 2015; 35:939–955. [PubMed: 25547292]
42. Ralser M, Wamelink MM, Struys EA, Joppich C, Krobitsch S, Jakobs C, Lehrach H. A catabolic block does not sufficiently explain how 2-deoxy-D-glucose inhibits cell growth. Proceedings of the National Academy of Sciences. 2008; 105:17807–17811.
43. de Diego RP, Sancho-Shimizu V, Lorenzo L, Puel A, Plancoulaine S, Picard C, Herman M, Cardon A, Durandy A, Bustamante J. Human TRAF3 adaptor molecule deficiency leads to impaired Toll-like receptor 3 response and susceptibility to herpes simplex encephalitis. Immunity. 2010; 33:400–411. [PubMed: 20832341]
44. Zhang S-Y, Jouanguy E, Ugolini S, Smahi A, Elain G, Romero P, Segal D, Sancho-Shimizu V, Lorenzo L, Puel A. TLR3 deficiency in patients with herpes simplex encephalitis. science. 2007; 317:1522–1527. [PubMed: 17872438]
45. Casrouge A, Zhang S-Y, Eidenschenk C, Jouanguy E, Puel A, Yang K, Alcais A, Picard C, Mahfoufi N, Nicolas N. Herpes simplex virus encephalitis in human UNC-93B deficiency. Science. 2006; 314:308–312. [PubMed: 16973841]
46. Sancho-Shimizu V, de Diego RP, Jouanguy E, Zhang S-Y, Casanova J-L. Inborn errors of anti-viral interferon immunity in humans. Current opinion in virology. 2011; 1:487–496. [PubMed: 22347990]
47. Sancho-Shimizu V, Zhang S-Y, Abel L, Tardieu M, Rozenberg F, Jouanguy E, Casanova J-L. Genetic susceptibility to herpes simplex virus 1 encephalitis in mice and humans. Current opinion in allergy and clinical immunology. 2007; 7:495–505. [PubMed: 17989525]
48. Lundberg P, Ramakrishna C, Brown J, Tyszka JM, Hamamura M, Hinton DR, Kovats S, Nalcioglu O, Weinberg K, Openshaw H. The immune response to herpes simplex virus type 1 infection in susceptible mice is a major cause of central nervous system pathology resulting in fatal encephalitis. Journal of virology. 2008; 82:7078–7088. [PubMed: 18480436]
49. Wang JP, Bowen GN, Zhou S, Cerny A, Zacharia A, Knipe DM, Finberg RW, Kurt-Jones EA. Role of specific innate immune responses in herpes simplex virus infection of the central nervous system. Journal of virology. 2012; 86:2273–2281. [PubMed: 22171256]

50. Kurt-Jones EA, Chan M, Zhou S, Wang J, Reed G, Bronson R, Arnold MM, Knipe DM, Finberg RW. Herpes simplex virus 1 interaction with Toll-like receptor 2 contributes to lethal encephalitis. Proceedings of the National Academy of Sciences of the United States of America. 2004; 101:1315–1320. [PubMed: 14739339]

Abbreviations

2DG	2-Deoxy-Glucose
HSV	Herpes Simplex Virus
HSE	Herpes Simplex Encephalitis
Pi	post infection
SK	Stromal Keratitis

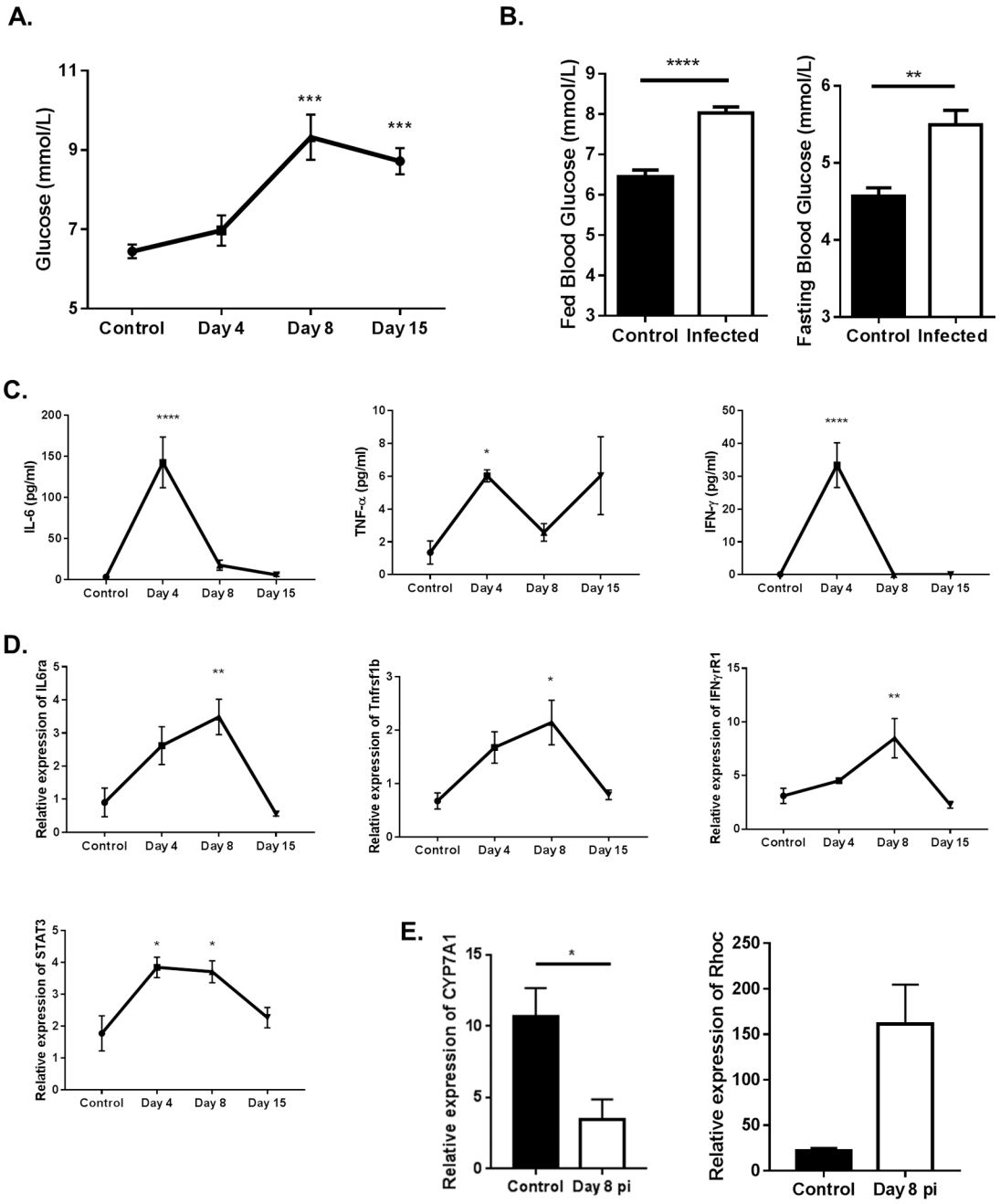

Figure 1. Blood glucose levels increase upon infection with HSV-1

C57BL/6 animals were either infected with 1×10^4 PFU of HSV-RE or left alone. (A,B) Blood glucose levels were measured at time points indicated post infection. (A) Line graph showing kinetics of blood glucose levels (fed state) in control, day 4, day 8 and day 15 pi. (B) Histogram showing fed state and fasting state blood glucose levels at day 15 pi. (C) Line graph showing changes in serum cytokine levels at different time points pi. (D) Line graph showing changes in gene expression in the liver at different time points pi. (E) Histogram representing the expression of CYP7A1 and RHOC in liver of naïve and day 8 pi animals. Data represents the mean ± SEM of more than 8 independent experiments for A, B (n = 5–8

mice/group) and 2 independent experiments for C-E (n=4–5 mice/group). Data were analyzed with One-way ANOVA for A, C & D compared to the control or student's t-test for B & E. P≤ 0.0001 (****), P≤0.001(***), P≤0.01(**), P≤0.05(*).

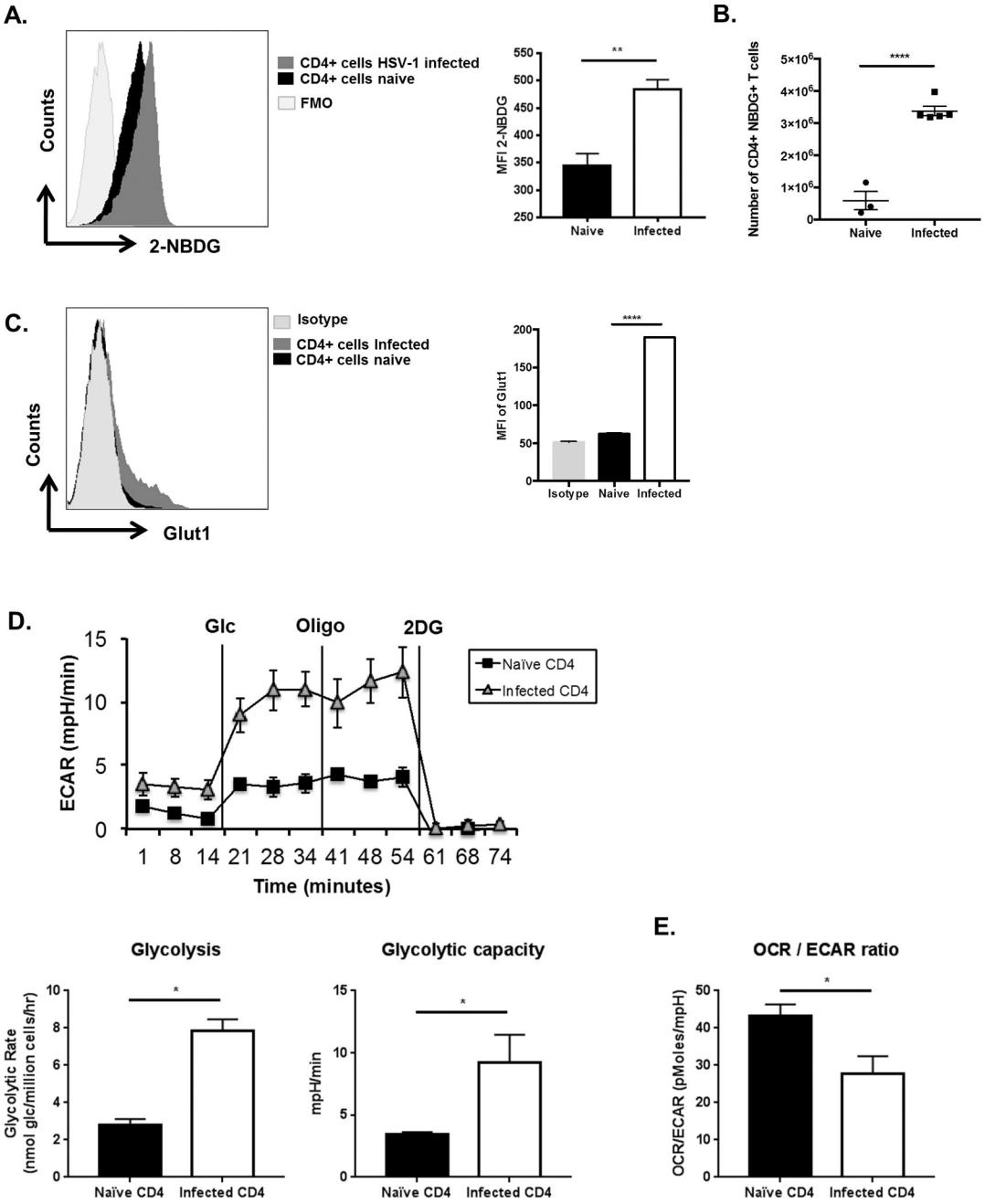

Figure 2. Glucose uptake in CD4 T cells increases at day 15 post infection

(A–E) C57BL/6 animals were either infected with 1×10^4 PFU of HSV-RE or left uninfected. (A, B) At day 15 pi animals showing SK lesions and naïve un-infected animals were administered with 2-NBDG (i.v) and glucose uptake by CD4 T cells was measured in DLNs. (A) Representative FACS plots and histogram (MFI) showing the 2-NBDG uptake by CD4 T cell from day 15 pi or naïve animals. For fluorescence minus one (FMO), mice were not injected with 2-NBDG. Cells were gated on live CD4+ T cells (B) Histogram number of CD4 T cells in DLNs with 2-NBDG uptake. (C) DLN from naïve and day 15 pi were stained with CD4 and Glut1 or Isotype. Representative FACS plots with Isotype control and

Histogram (MFI) showing GLUT-1 expression by CD4 T cells. Cells were gated on live CD4+ T cells (D, E) Total CD4 T cells were purified from naïve and day 15 pi mice showing SK lesions and equal number of cells were used of extracellular flux analysis (D) Line graph showing changes in Extracellular acidification rates (ECAR) by CD4 T cells following addition of glucose, oligomycin and 2DG and Histograms showing basal glycolysis, glycolytic capacity (E) Histogram showing the ratio of OCR to ECAR. Data represents the mean ± SEM of more than 3 independent experiments for A–C (n = 3–5 mice/group) and 2 independent experiments for D & E (n=5 replicates/group). All the data were analyzed with student's t test. P≤ 0.0001 (****), P≤0.01(**), P≤0.05(*)

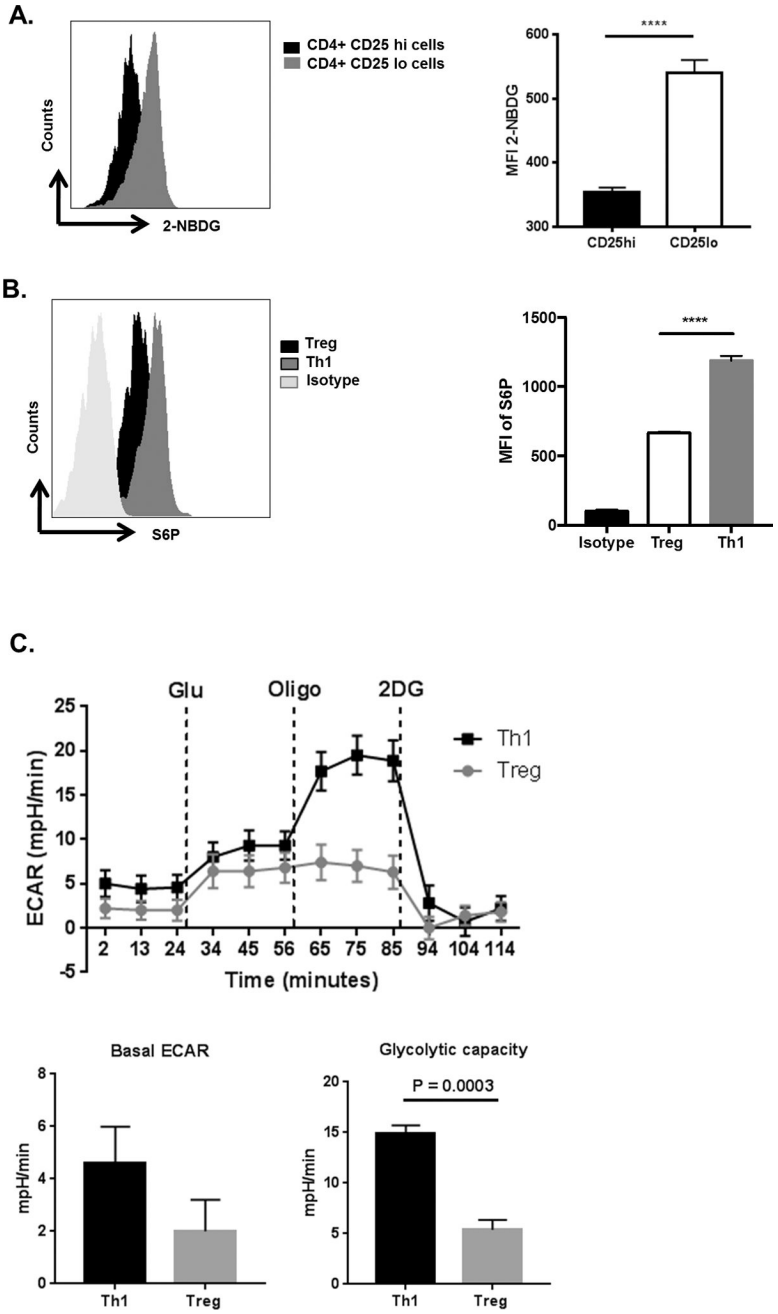

Figure 3. CD4 T cells from infected and naïve animals have different glucose metabolism

(A) C57BL/6 animals were infected with 1×10^4 PFU of HSV-RE and at day 15 pi animals showing SK lesions were administered with 2-NBDG (i.v) and glucose uptake by different CD4 T cell subsets was measured in DLNs. Representative FACS plots and histogram (MFI) showing the 2-NBDG uptake in Live cells of Treg (CD4+CD25+) cells and Teff (CD4+CD25−) cells as measured in DLNs at day 15 pi. (B) DLNs at day 15 pi were stimulated PMA/Ionomycin followed by ICS assay. Representative FACS with Isotype control and histogram (MFI) of S6P in Treg (CD4+ Foxp3+) and Th1 (CD4+ IFN-γ+) cells. Dead cells were gated out using Live/Dead staining. Data represents the mean ± SEM of

more than 3 independent experiments (n = 3–5 mice/group) (C) Naive CD4 T cells purified from C57BL/6 mice were cultured in either Treg or Th1 differentiating conditions. After 5 days, equal number of cells were used of extracellular flux analysis. Line graph showing changes in extracellular acidification rates (ECAR) by CD4 T cells following addition of glucose, oligomycin and 2DG and Histograms showing basal ECAR and glycolytic capacity. Data represent the mean values ± SEM of two independent experiments of n = 4. The level of significance was determined by Student's t test (unpaired). P≤ 0.0001 (****)

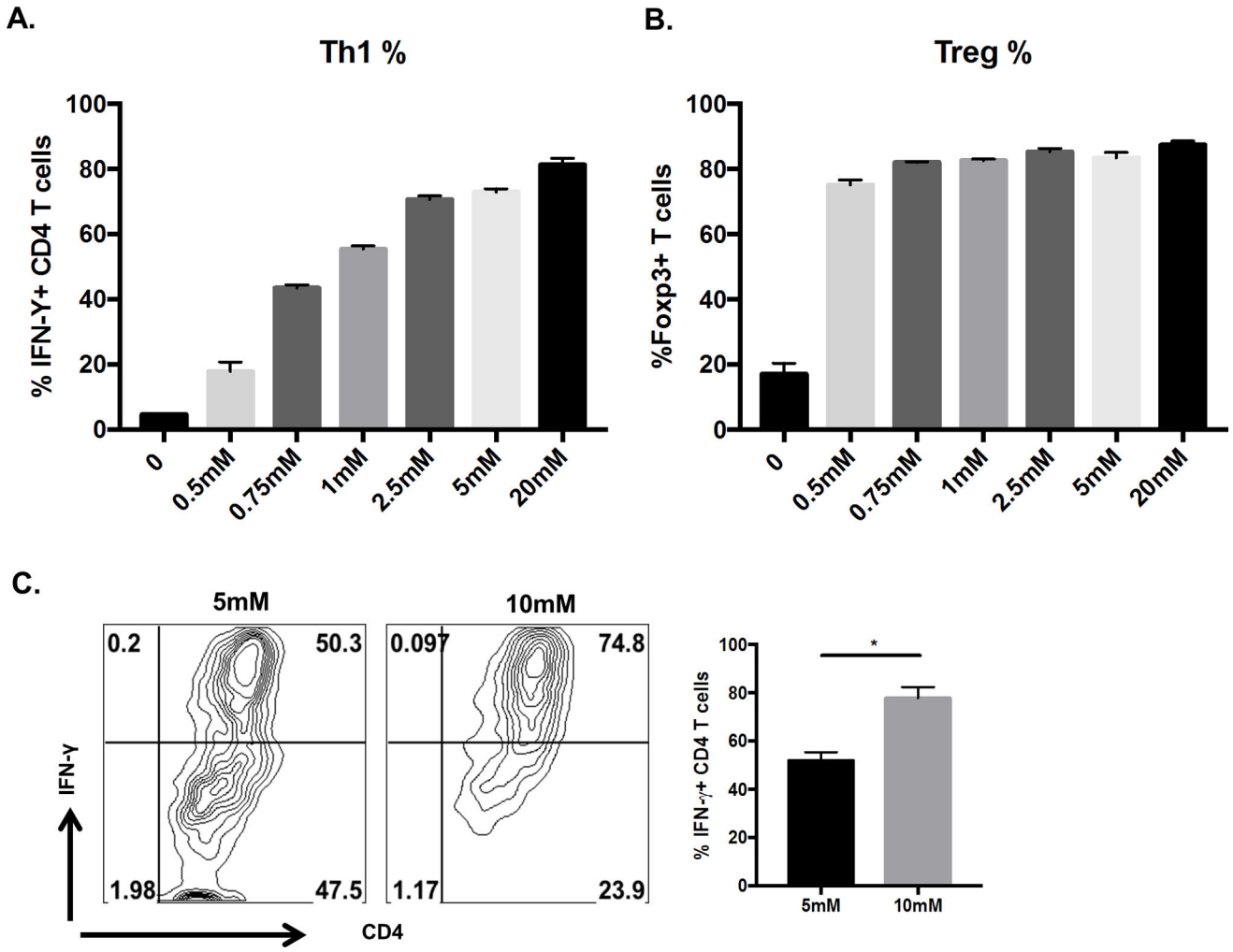

Figure 4. Increasing glucose levels increases Th1 but not Treg differentiation

Splenocytes from DO11.10 RAG2−/− mice were cultured (1 million cells) in the presence of 1 μg/ml of anti-CD3/CD28 antibody with either 100 U/ml of recombinant IL-2, 1ng/ml TGF-β (Treg differentiating conditions) or IL-12 (5ng/ml), anti-IL-4 (10 μg/ml) (Th1 differentiating conditions) with increasing concentrations of glucose(0.5mM–20mM) in glucose free conditions (A) Histogram showing frequency of IFN-γ during Th1 differentiation or (B) Foxp3 expression during Treg differentiation with increasing glucose concentrations (C) Representative FACS plots and histogram showing IFN-γ expression under Th1 differentiating conditions in the presence of glucose concentrations (5mM and 10mM). Cells were gated on live CD4+ T cells. Data represents means ± SEM from three independent experiments (n = 3/group). The level of significance was determined by Student's t test (unpaired) P≤0.05(*).

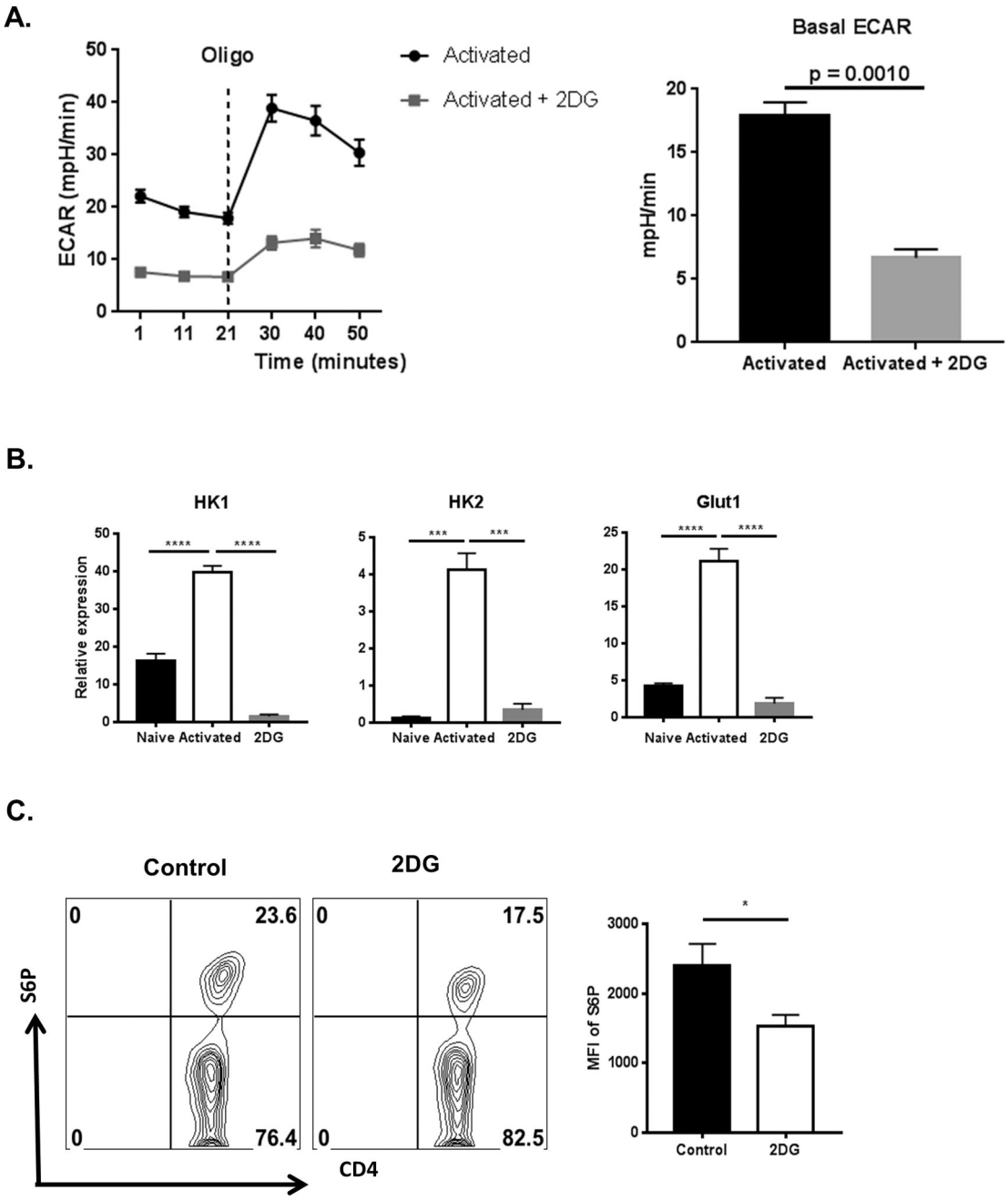

Figure 5. 2DG inhibits the metabolic reprogramming of CD4 T cells following activation

(A) Naive CD4 T cells purified from C57BL/6 mice were cultured (500,000 cells/well) with 100U/ml IL-2, 1μg/ml anti-CD3/CD28 and in the presence or absence of 250μM 2DG for 3 days followed by extracellular flux analysis. Line graph showing changes in Extracellular acidification rates (ECAR) by CD4 T cells following addition of oligomycin and Histograms showing basal ECAR levels. (B) Naive CD4 T cells purified from C57BL/6 mice were cultured (100,000 cells/well) with 1μg/ml anti-CD3/CD28 and in the presence or absence of 250μM 2DG for 24 hours followed by gene expression analysis by QRT-PCR compared to beta-actin. Histogram representing expression of genes involved in glucose metabolism such

as HK1, HK2 and Glut1 in naïve, activated and Activated in the presence of 2DG (2DG). (C) Naïve CD4 T cells were cultured (100,000 cells/well) with 1μg/ml anti-CD3/CD28 in the presence or absence of 250μM 2DG for 24 hours followed by measurement of Phosphorylation of S6 using flow cytometry. Representative FACS plots and histogram (MFI of S6P) of live CD4 T cells. Data represents means ± SEM from two independent experiments (n = 3/group) and the level of significance was determined by Student's t test (unpaired) for A & C and One-way ANOVA for B. P≤ 0.0001 (****), P≤0.001(***), P≤0.01(**), P≤0.05(*).

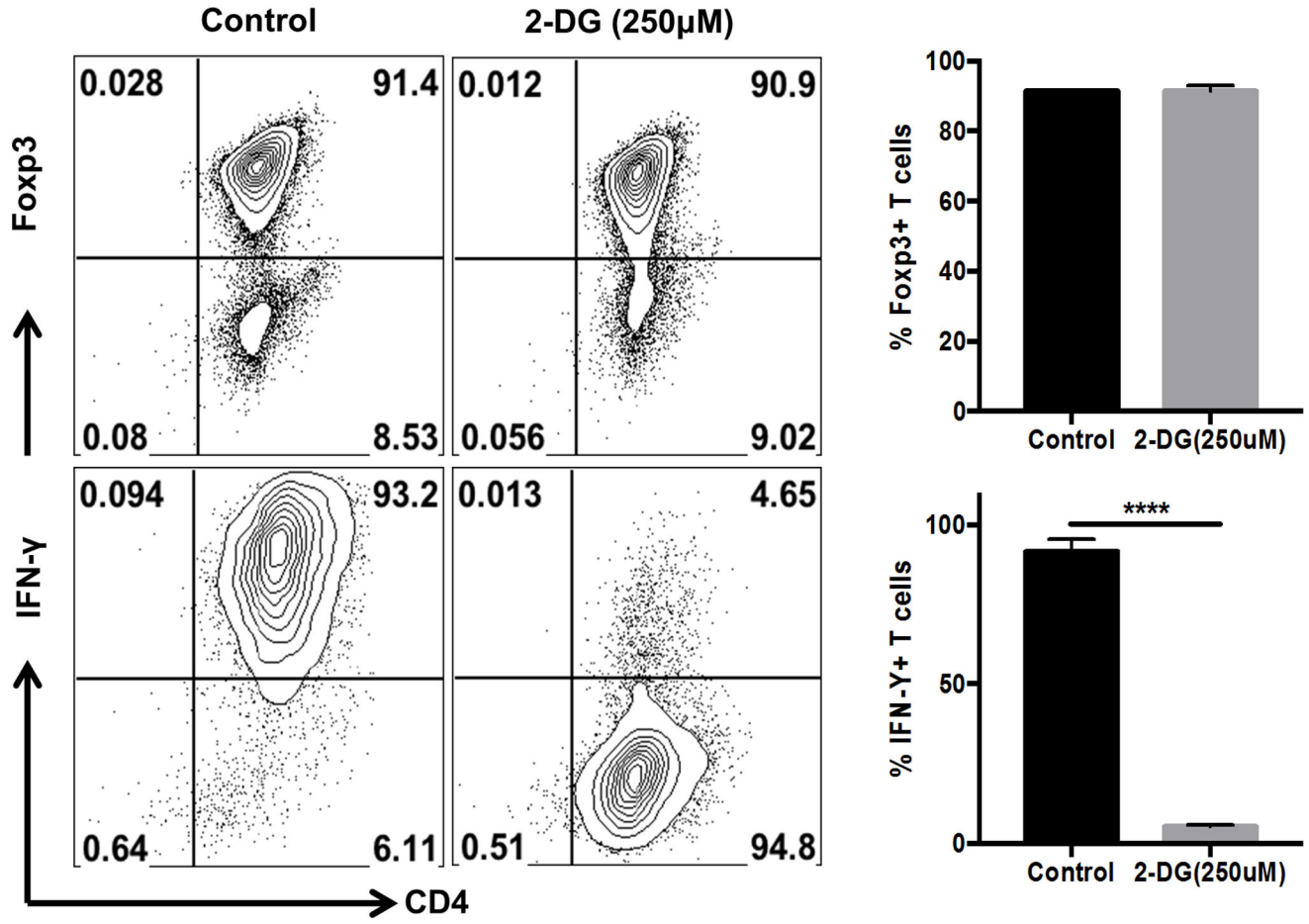

Figure 6. Effect of 2DG treatment on glycolysis and T cell differentiation

Splenocytes from DO11.10 RAG2−/− mice were cultured (1 million cells) in the presence of 1 μg/ml of anti-CD3/CD28 antibody with either 100 U/ml of recombinant IL-2, 5ng/ml TGF-β (Treg differentiating conditions) or IL-12 (5ng/ml), anti-IL-4 (10 μg/ml) (Th1 differentiating conditions) with or without 2DG (250μM). After 5 days of culture, cells were analyzed for the expression of IFN-γ and Foxp3 on CD4 T cells. Representative FACS plots and histogram showing the frequency of Th1 and Treg. Cells were gated on live CD4+ Foxp3+ T cells (Treg) and live CD4+ IFN-γ + T cells (Th1). Data represents means ± SEMs of three independent experiments with n=3/group. Statistical significance was calculated by Student's t test (unpaired) P≤ 0.0001 (****).

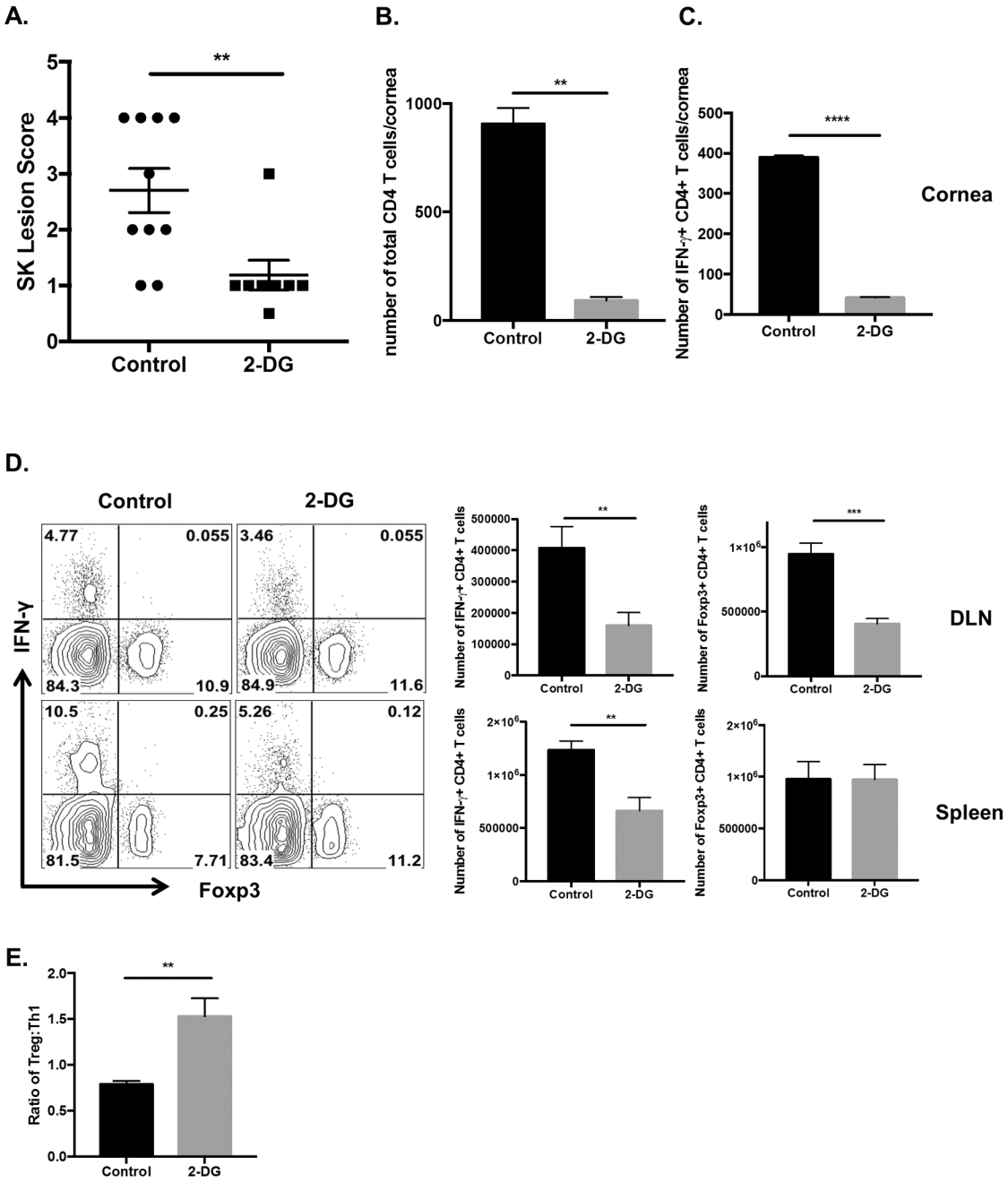

Figure 7. Therapeutic administration of 2DG diminishes SK severity

C57BL/6 animals infected with 1×10^4 PFU of HSV-RE were given either 2DG or PBS from day 5 pi to day 14 pi. The disease progression was analyzed in a blinded manner using a scale described in materials and methods. (A) Individual eye scores of SK lesion severity on day 15 pi. (B) Representative histogram showing the number of total $CD4^+$ T cells infiltrating the cornea at day 15 p.i (C) Pool of corneas were stimulated with PMA/ Ionomycin, representative histogram showing the number of Th1 (Live CD4+ IFN-γ) cells in the cornea at day 15 pi. (D) DLN and Spleen were stimulated with PMA/Ionomycin, representative FACS plots and histogram showing frequency and number of Treg (live CD4+

Foxp3+) and Th1 (live CD4+ IFN-γ). (E) Histogram representing Treg to Th1 ratio in the spleen at day15 pi. Data represents the mean ± SEM of more than 3 independent experiments (n=3–10 mice/group). All the data were analyzed with student's t test. P≤ 0.0001 (****), P≤0.001(***), P≤0.01(**)

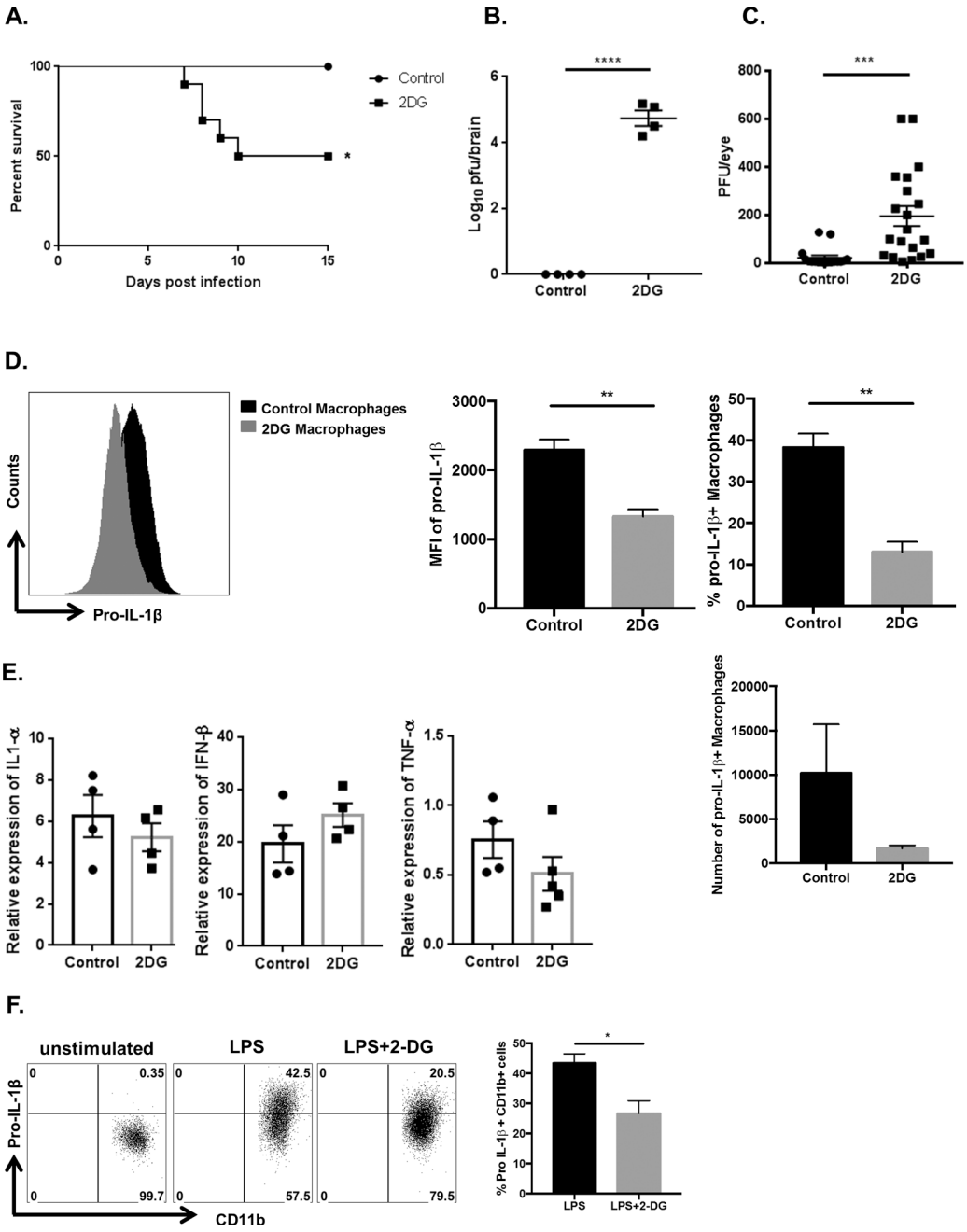

Figure 8. 2DG administration during early HSV infection is lethal

C57BL/6 animals infected with 1×10^4 PFU of HSV-RE were given either 2DG or PBS from day 0 pi to day 15 pi. (A) Survival of 2DG and control treated was established over 15 days. (B) Brains were harvested from 2DG treated and control mice at day 10 pi and homogenized, centrifuged, and the supernatants were tested for virus titers using plaque assay. (C) The presence of virus in the cornea was measured at day 6 pi by swabbing the HSV infected eye with a sterile swab and assaying for the virus by plaque assay. (D) Corneas were isolated at day 2 pi from control and 2DG treated animals and inflammatory macrophages (CD45+ CD11b+ F4/80+ Pro-IL-1β+) were identified using flow cytometry.

Representative FACS plots and histogram showing MFI of pro-IL-1β, frequency and number of inflammatory macrophages in corneas of 2DG treated and control animals at day 2 pi. (E) Corneas were isolated from control and 2DG treated animals at day 2 pi and RNA was isolated followed by gene expression analysis by QRT-PCR. Histogram representing the gene expression of IL-1α, IFN-β and TNF-α. (F) Bone marrow derived macrophages (BMDM) were differentiated from naïve bone marrow progenitor cells (as described in materials and methods). BMDMs were stimulated with LPS (20ng/ml) in the presence or absence of 2DG (250μM) for 24 hours. Representative FACS plots and histogram showing frequency of BMDM expressing Pro-IL-1β (CD45+ CD11b+ F4/80+ Pro-IL-1β+). Data represents mean values ± SEM (n = 4–8 mice/group) for A–F. Experiments were repeated at least three times. The level of significance was determined by Student's t test (unpaired). P≤ 0.0001 (****), P≤0.01(**), P≤0.05(*).